Dynamic modeling of compressed gas energy storage to complement renewable wind power intermittency

Jean-Paul Maton, Li Zhao, Jacob Brouwer*

Advanced Power and Energy Program, University of California, Irvine, CA 92697-3550, USA

ARTICLE INFO

ABSTRACT

To evaluate the impacts and capabilities of large-scale compressed gas energy storage for mitigating wind intermittency, dynamic system models for compressed air energy storage and compressed hydrogen energy storage inside salt caverns have been developed. With the experimental data from air storage in a salt cavern in Huntorf, Germany, the cavern model has been verified. Both daily and seasonal simulation results suggest that with the same size wind farm and salt cavern, a compressed hydrogen energy storage system could better complement the wind intermittency and could also achieve load shifting on a daily and seasonal time scale. Moreover, the hydrogen produced in the compressed hydrogen energy storage system could also be dispatched as a fuel to accommodate zero emission transportation for up to 14,000 fuel cell vehicles per day while achieving seasonal load shifting.

1. Introduction

With increasing energy demand and growing concerns for environmental impacts, renewable energy sources are receiving increased attention for their inherent low pollutant and greenhouse gas emissions. Over the past few years, renewable wind power has become one of the fastest growing sectors of the U.S. renewable energy portfolio [1,2]. In 2010, wind power installation in the U.S. was roughly 5 GW and comprised 25% of U.S. electric generating capacity additions [2]. In addition, 12,100 MW of new wind capacity is expected to be added by the year 2013, with forecasts of meeting 20% of the nation's electricity demand from wind energy by the year 2030 [2]. However, the intermittent and uncontrollable nature of wind power sources introduces new technical challenges for integration into electric power systems, especially as the market share of wind power becomes large. Wind power is

intermittent directly due to spatial and temporal wind speed variations [3]. Spatial variability of wind speed is introduced by various climate regions, geographical location, local vegetation and topography [3]. Temporal intermittency and variability of wind power includes typical annual and seasonal variations, synoptic, diurnal and turbulence variations. Due to these uncontrollable intermittencies that act in different time scales, wind power sources could have significant negative impacts on grid operation in different time scales, including those that affect regulation, load following, and scheduling [3–5]. In the time scale of regulation (seconds to minutes), the impact of the wind intermittency may require significantly more regulation reserves and frequency control [5,6]. In the load following time scale (minutes to hours), wind intermittency may require a significant increase in the amount of operating reserves [6]. In the scheduling time scale (hours to days), the wind intermittency may result in significant economic costs due to

Nomenclature			
m_{cavern}	mass of gas in the cavern	A	inner surface area of the cavern
$\dot{m}_{in}$	rate of mass flow into cavern	r_1	average radius of the cavern
$\dot{m}_{out}$	rate of mass flow out of cavern	r_2	radial distance to reach equilibrium with surrounding salt
U_{cavern}	internal energy of the cavern	L	the height of the cavern
$\dot{n}$	molar rate of gas flow entering or exiting the cavern	k	thermal conductivity of salt (NaCl) as a function of temperature
$\bar{h}_{in}$	molar specific enthalpy of the gas entering the cavern	Nu_D	Nusselt number
$\bar{h}_{out}$	molar specific enthalpy of the gas exiting the cavern	Re_D	Reynolds number
		Pr	Prandtl number
$\dot{Q}_{in}$	rate of heat transfer into the cavern	$\bar{s}$	molar specific entropy
T_{surr}	temperature of the surrounding bedded salt	$\Delta\bar{h}$	change in molar specific enthalpy
T_{cavern}	temperature of the gas inside the cavern	P	pressure
R_{conv}	thermal resistance for convective heat transfer	T	temperature
R_{cond}	thermal resistance for conductive heat transfer	R_u	universal gas constant
h	convection coefficient	$\bar{c}_p(T)$	constant pressure specific heat as a function of temperature

disturbing the generation mix versus time across the whole generation portfolio [3,6]. At the current trends, higher renewable wind power penetration will occur and the large-scale integration needs to be implemented to accommodate the increased wind power penetration. To deal with the increased variability introduced by large-scale wind power generation on the power systems, several methods are proposed to complement the wind power intermittency and to improve the ability to integrate the increasing wind capacity. Methods focused on demand side management such as demand response technologies are being considered to reduce and manage the wind intermittency [7,8]. Improvements in the operational flexibility of conventional power plants will also complement the intermittency of wind power [3,4]. But with high market adoption of wind power it is expected that these measures alone will not be able to fully complement wind power, nor can these measures store wind power that would otherwise be curtailed (i.e., when production exceeds demand). Introducing energy storage technologies is a promising option to manage and complement wind intermittency [6,7,9,10].

There are many different energy storage technologies currently available, each with its own advantages and constraints. Hydrogen energy storage, pumped hydro, compressed air energy storage, various types of battery systems, flywheels, super capacitors, and thermal energy storage are all either being used or investigated for integrating intermittent renewable energy. These energy storage systems can provide frequency regulation, alleviate transmission congestion, defer costs of new construction, provide load shifting, and/or reduce "time of use" and demand charges [11—14]. Over the past decade, many studies have been focused on modeling and analyzing the technical and economic implications of using energy storage technologies to integrate intermittent wind energy. Many of these studies were focused on small-scale applications such as stand-alone wind and energy storage systems [10,15—17]. For large scale integration and large capacity energy storage, the potential applications have been mainly focused upon pumped hydro energy storage, compressed air energy storage, and hydrogen energy storage [6,11,18—21], that could enable a larger storage capacity to accommodate massive energy storage for not only daily load shifting but also seasonal load shifting. Pumped hydro energy storage is the oldest and most widely used method of such massive energy storage, accounting for over 99% of energy storage worldwide. A location with a suitable elevation gradient to provide the gravitational potential energy, and a large amount of storage media (water) are required to achieve large scale pumped hydro energy storage [9,21]. Compared to pumped hydro energy storage, compressed gas (air/hydrogen) energy storage systems will require much less water and do not require a large elevation gradient. Compressed gas energy storage systems typically use existing underground sites (e.g., a salt cavern), and will have the potential advantage of higher energy storage capacity and much lower cost than batteries and ultra-capacitors, since the amount of stored energy is decoupled from the energy conversion device size [6]. A 2.25 GW rated integrated compressed air renewable energy system has been examined by Garvey et al. [22]. Performance measures of the system simulation indicated that effective turnaround efficiency is over 85% and the wholesale value of the output power may be increased by a factor of 1.3 [22]. Worldwide there are currently two compressed air energy storage facilities in operation, one in Huntorf, Germany, and one in McIntosh, Alabama [23]. To release the stored energy the compressed air is routed to a gas turbine that is also fueled by natural gas to produce electricity. One of the challenges that have plagued recent compressed air energy storage systems is associated with the operation and emissions from high pressure combustion [23]. A model for compressed air energy storage inside caverns has been developed by Raju and Khaitan that simulates the mass and energy balance inside the storage cavern and has been verified with the Huntorf facility, but the dynamics associated with the system were not simulated or discussed [24].

A compressed hydrogen energy storage system typically has an electrolyzer that produces hydrogen from water by using wind energy, and a hydrogen fuel cell that utilizes the hydrogen to provide power to the grid. Compressed hydrogen energy storage has been considered less favorable due to its low round trip efficiency and relatively high cost [25].

However, for integration with large-scale wind energy, large energy capacity and low self-discharge become more important than round trip efficiency [6], therefore compressed hydrogen energy systems with electrolyzers and fuel cells become more attractive as the amount of energy storage required increases. Compressed hydrogen energy storage has been demonstrated by NREL and Xcel Energy with the Wind-to-Hydrogen demonstration project in Boulder, Colorado. In the most recent demonstration, low temperature electrolysis is applied using a proton exchange membrane (PEM) electrolyzer to split water into hydrogen. The PEM electrolyzer achieved a system efficiency of 57% [26]. Moreover, hydrogen energy storage has the additional, synergistic benefit that the hydrogen produced using wind power (that would have otherwise been curtailed) could also be used as a renewable domestic fuel to enable completely zero emission transportation. Gonzalez et al. showed that hydrogen energy storage could drastically increase wind energy penetration since hydrogen produced from excess wind could be used for purposes other than electricity [27].

To further understand the dynamics of compressed air and hydrogen energy storage technologies integrated with large-scale wind power and their impacts on the grid, dynamic system models have been developed and verified for compressed air and hydrogen energy storage systems in this study. A hypothetical wind farm has also been modeled and integrated with measured demand profiles and the dynamic compressed air and compressed hydrogen energy storage models. In this overall system model, the implemented energy storage transforms the intermittent renewable resource into a power plant that can produce dispatchable power. The compressed gas energy storage acts to buffer the intermittent nature of wind power. Dynamics associated with wind power/demand fluctuations, timescale variations, hydrogen and compressed air conversion technologies, and storage size variations are simulated and discussed.

2. Model development

2.1. Methodology

To analyze the implications of compressed gas energy storage systems, a detailed system model comprised of a wind farm, energy storage system and the grid is developed in MATLAB/Simulink®. The performance of a hypothetical wind farm in combination with an energy storage system with an underground salt cavern forms the basis of comparison between two energy storage methods: compressed air energy storage and compressed hydrogen energy storage. When the power generated by the wind turbines exceeds the load on the grid, the excess wind power is diverted to produce gas storage in the cavern. If the wind power is insufficient to meet the load, the energy in storage is released to meet the demand. It is assumed that sufficient equipment is available to capture all excess wind power for storage, and also to generate the necessary power to meet demand when the wind power is too low. Ten-minute dynamic resolution is adopted in the current study. Both daily and seasonal load shifting capabilities are investigated using the model. Moreover, the scenario in which hydrogen produced

is synergistically dispatched as fuel to accommodate zero emission transportation is also investigated.

2.2. Model components

2.2.1. Wind farm
Wind power is modeled using a wind farm model that uses wind speed data with 10 min resolution that was obtained from the Wind Integration Datasets provided by the National Renewable Energy Laboratory and 3TIER. The wind speed datasets indicate an area of excellent wind potential in northern Texas about 30 miles east of the city of Plainview. Wind speed fluctuations are not uniformly distributed over an entire area, with wind gusts affecting some turbines but not others. Counterbalancing gusts may increase the power output of some parts of the wind farm while at the same time decrease the output of other parts. Gathering data from only one or two unique locations may not fully capture the dynamics of a particular wind farm power output [1]. Therefore, wind speeds were obtained from 50 individual grid points uniformly distributed over approximately 100 square miles in the Plainview, TX region for the current study. These multiple grid points were used in order to more accurately represent the actual power output of an entire wind farm (or several aggregate wind farms) spread out over a fairly large region. Power derived from the wind is determined using Equation (1):

$$Power = COP * \frac{1}{2}\rho A v^3 \tag{1}$$

where COP is a coefficient of performance used to match a particular wind turbine's power curve, ρ is the density of air, A is the area of the circle swept out by the turbine blades, and v is the velocity of the wind. Vestas V164-7 MW wind turbines with a cut-in wind speed of 4 m/s and a cut-out wind speed of 25 m/s were used in the Texas wind farm model of this study.

2.2.2. Electric grid
Electric grid demand was obtained from the Electric Reliability Council of Texas (ERCOT). ERCOT services 85% of the state's electric load [28]. The demand for the entire ERCOT region in the year 2006 was obtained with 15-min resolution. The demand profile has been scaled down for matched use with a 200 turbine wind farm (total rated power of 1400 MW), corresponding to wind power meeting roughly 2% of the total annual demand.

2.2.3. Underground salt cavern
A solution mined salt cavern has been modeled for the compressed gas energy storage systems simulated in this paper. Lower pressure underground gas storage in bulk quantities is much less expensive than above ground storage in high pressure containers. For hydrogen, underground gas storage is also less expensive than storing in liquefied form [29]. For many decades, various types of underground geologies have been exploited for geologic storage of compressed gas. Depleted oil and natural gas wells, aquifers, mined hard rock caverns, and solution mined salt caverns have all been utilized. Recent studies have been conducted to evaluate various types of geology for storage, and the results show that salt caverns provide the lowest risk of gas leakage, provide

customizable cavern sizes, can be cycled (charged and discharged) more frequently than depleted oil and gas wells or aquifers, and require a smaller amount of cushion gas for operation [29–31]. In fact, the three underground hydrogen storage facilities as well as the two compressed air energy storage facilities currently in operation all utilize solution mined salt caverns.

The minimum and maximum pressures of the storage cavern are dependent upon the local geology among other things. For the simulations presented in this paper, a minimum and a maximum pressure of 45 bar and 135 bar, respectively, were used. A cushion gas (which generally establishes the minimum pressure) is required to produce a residual pressure that allows for the extraction of the working gas [30]. In depleted oil and natural gas wells up to 50% (as high as ∼80% for aquifers) of the gas may be cushion gas and not useable for energy storage. Salt caverns tend to require less cushion gas (∼30%) [31].

In order to simulate the dynamics of cavern pressure and temperature as it is charged and discharged, the salt cavern and associated piping are taken as a control volume in the model developed. Mass and energy balances are calculated within MATLAB/Simulink® with the following dynamic equations:

$$\frac{dm_{cavern}}{dt} = \dot{m}_{in} - \dot{m}_{out} \qquad (2)$$

$$\frac{dU_{cavern}}{dt} = \dot{n}\bar{h}_{in} - \dot{n}\bar{h}_{out} + \dot{Q}_{in} \qquad (3)$$

where m_{cavern} is the mass of the gas in the cavern, $\dot{m}_{in}$ and $\dot{m}_{out}$ are the mass flow rates in and out of the cavern, U_{cavern} is the internal energy of the cavern, $\bar{h}$ is the molar specific enthalpy of the gas entering or exiting the cavern, $\dot{n}$ is the molar flow rate of the gas entering or exiting the cavern, and $\dot{Q}_{in}$ is the rate of heat transfer into the cavern.

To determine the heat transfer ($\dot{Q}_{in}$), the cavern is modeled as a cylinder with one dimensional radial heat transfer using a thermal resistance for convection and conduction as shown in Equations (4)–(7):

$$\dot{Q}_{in} = \frac{\Delta T}{R_{total}} \qquad (4)$$

$$R_{total} = R_{conv} + R_{cond} \qquad (5)$$

$$R_{conv} = \frac{1}{hA} \qquad (6)$$

$$R_{cond} = \frac{\ln(r_2/r_1)}{2\pi Lk} \qquad (7)$$

where ΔT is the temperature difference between the surrounding bedded salt (T_{surr}) and the gas inside the cavern (T_{cavern}), R_{conv} is the thermal resistance for convective heat transfer, R_{cond} is the thermal resistance for conductive heat transfer, h is the convection coefficient, A is the inner surface area of the cavern, r_1 is the average radius of the cavern, r_2 is the radial distance to reach equilibrium with surrounding salt, L is the height of the cavern, and k is the thermal conductivity of salt (NaCl) as a function of temperature.

For the heat loss through the walls of the cavern, the convection term is limited to natural convection. Within the cavern the velocity of gas flow during charging and discharging is minimal due to the enormous size of the salt cavern in proportion to flow rates in or out of the cavern. Thus, convective heat transfer in the cavern is assumed to be negligible. On the other hand, heat loss through the piping that connects the underground cavern to the above ground equipment is modeled with forced convection due to the rapid flow through pipes with a relatively narrow diameter. A method for determining heat transfer in underground caverns introduced by Raju and Khaitan is adopted to correlate the forced convection heat transfer with the mass flow entering or leaving the cavern [24]. It is based on the Dittus–Boelter equation for fully developed turbulent flow through tubes, where Nu_D is the Nusselt number, Re_D is the Reynolds number, and Pr is the Prandtl number.

$$Nu_D = 0.023 Re_D^{0.8} Pr^n \qquad (8)$$

Derived from the Reynolds number, the Nusselt number (and the forced convection coefficient h) can be related to the mass flow through the pipes using Equations (9) and (10):

$$Nu_D \propto |\dot{m}_{in} - \dot{m}_{out}|^{0.8} \qquad (9)$$

$$h_{conv,forced} \cong b_{conv}|\dot{m}_{in} - \dot{m}_{out}|^{0.8} \qquad (10)$$

The model parameter b_{conv} is determined by verifying the simulation results with the experimental data from the Huntorf compressed air energy storage system (see model validation in the next section).

2.2.4. Compressed air energy storage

A compressed air energy storage system normally uses excess electricity to run air compressors and stores high pressure air in tanks or underground caverns. To release the stored energy the compressed air is routed to a gas turbine fueled by natural gas that produces electricity. This energy storage system requires a substantial amount of fossil fuel to operate and therefore carbon dioxide emissions can be generated by the system. Worldwide there are currently two compressed air energy storage facilities in operation. One in Huntorf, Germany [32], and the other in the United States located in McIntosh, Alabama. Because of difficulties with high pressure combustion, as well as size limitations of the customized equipment used at the McIntosh plant, the next generation of compressed air energy storage systems have adopted a new strategy [23]. One of the many variations of these new systems has been adapted for the simulation undertaken in this paper. Fig. 1 shows the schematic of the compressed air energy storage system.

When excess wind power is available atmospheric air is compressed and stored in an underground salt cavern. In power production mode a conventional combustion gas turbine provides power and heat. The hot exhaust gases are channeled through a recuperator in order to heat the compressed air as it is released from storage. The compressed air from storage then passes through high pressure and low pressure expanders before being expelled into the atmosphere. Air injection refers to a portion of the air flow that is
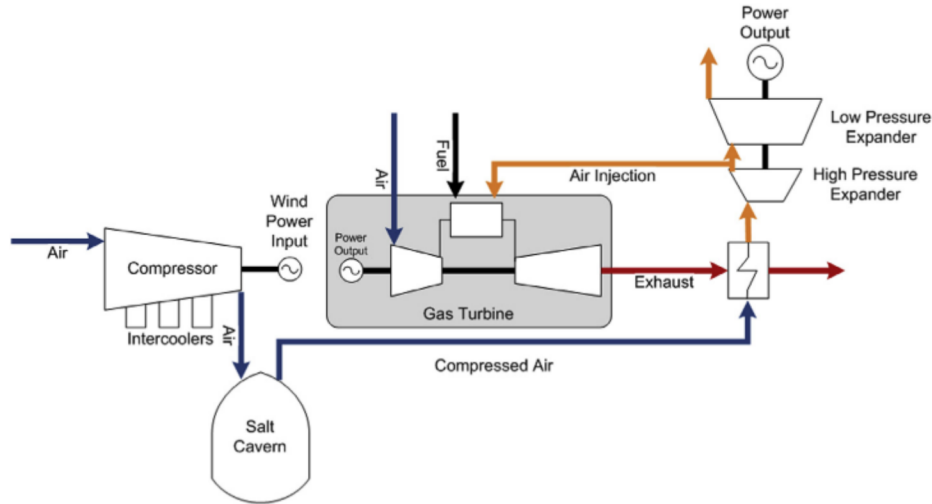
Fig. 1 – Schematic of compressed air energy storage system with air injection.

diverted from the exhaust of the high pressure expander and is directed to the combustion turbine in order to reduce the load on its compressor and increase its efficiency. Power for compression and from expansion of gases is derived from enthalpy changes using Equation (11):

$$Power = \dot{n}\Delta\bar{h} \tag{11}$$

Changes in enthalpy are derived from isentropic relations (adjusted by realistic isentropic efficiencies for compressors and turbines). With a known inlet temperature and change in pressure, the exit temperature and $\Delta\bar{h}$ can be determined by Equations (12) and (13):

$$\bar{s}_{out} - \bar{s}_{in} = \int_{T_{in}}^{T_{out}} \frac{\bar{c}_p(T)}{T} - R_u \ln\left(\frac{P_{out}}{P_{in}}\right) \tag{12}$$

$$\Delta\bar{h} = \int_{T_{in}}^{T_{out}} \bar{c}_p(T)dT \tag{13}$$

2.2.5. Compressed hydrogen energy storage

In the hydrogen energy storage system excess energy from the wind farm is directed to electrolyzers that electrochemically split water into hydrogen and oxygen gas. The hydrogen is compressed and stored in the underground salt cavern. When power is required to meet the demand, the stored hydrogen is converted back to electrical energy in a proton exchange membrane (PEM) fuel cell. A small amount of power is derived from a turbine placed between the salt cavern and the fuel cell. The system schematic is shown in Fig. 2. Hydrogen can also be piped to urban areas for transportation or for use in distributed generation applications. The oxygen byproduct could also be collected and utilized for various applications such as biomass and coal gasification plants [33].

NREL's Wind-to-Hydrogen Project provided electrolyzer operational and efficiency data that were used to develop and calibrate the model [26]. Electrolysis is modeled as that occurring in PEM electrolyzers at an operating temperature of

55 °C, with an output pressure of 13.1 bar for hydrogen at the cathode, and 2 bar for oxygen at the anode. Using the Nernst Equation (14), the ideal stack voltage (per cell) of 1.48 V ($E°$) is adjusted to 1.52 V (E) [26]. In the following expression (14) R_u is the universal gas constant; T is the temperature of the electrolyzer stack; z is the number of moles of electrons transferred per mole of H_2; F is Faraday's constant; P_{H_2}, P_{O_2}, and P_{H_2O} are the partial pressures of hydrogen, oxygen, and water, respectively.

$$E = E° + \frac{R_u T}{zF} \ln\left(\frac{P_{H_2} P_{O_2}^{1/2}}{P_{H_2O}}\right) \tag{14}$$

This 1.52 V is the ideal voltage for the stated conditions of the Wind-to-Hydrogen project. Actual stack voltages ranged from 1.6 V to 2.2 V. The polarization curve, while affected by activation losses, exhibited mostly linear voltage dependence upon current due to ohmic losses within this range of operation. In addition to these electrochemical losses, there are
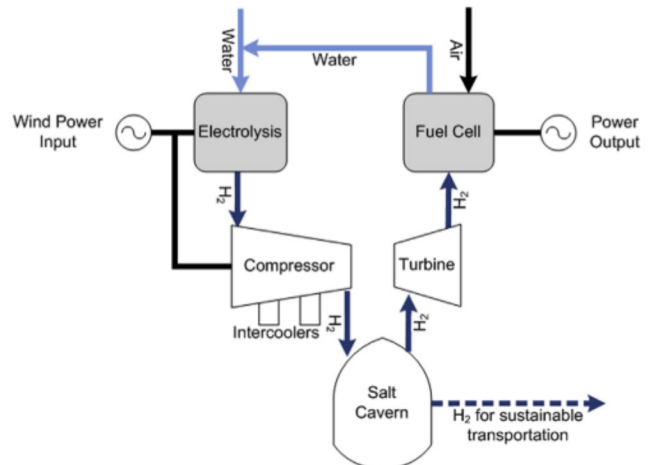

Fig. 2 – Schematic of compressed hydrogen energy storage system.

balance of plant (BOP) losses associated with pumps and fans to provide cooling and water management. In the current electrolyzer model voltage was verified to produce a polarization curve in the 1.6−2.2 V range with additional energy input added to account for BOP losses to match the system efficiency results reported by the Wind-to -Hydrogen Project [26].

A fuel cell system efficiency of 58% (LHV) was obtained from NREL's 2009 Technical Report on hydrogen technologies [21]. The actual cell voltages achieved by PEM fuel cells range between 0.6 V and 0.8 V per cell [34−36]. However, voltage is increased at pressures higher than 1 bar [36]. In the current model operating cell voltages were determined to be between 0.65 V and 0.85 V due to the fact that the hydrogen fuel comes from a high pressure compressed gas source.

Production and consumption of hydrogen is calculated with Faraday's Law:

$$I = zFN \qquad (15)$$

where I is the current, z is the number of moles of electrons transferred per mole of H_2, F is Faraday's constant, and N is the number of moles of hydrogen produced (or consumed) per second.

2.3. Assumptions

The following assumptions are made in the system model:

- Temperature of the compressed gas (air or hydrogen) entering the salt cavern has been cooled to 323 K by heat loss to the environment.
- Temperature of the salt basin surrounding the cavern is 318.5 K.
- Volume of the small salt cavern is 310,000 cubic meters.
- Volume of the large salt cavern is 3.8 million cubic meters.
- Maximum allowable cavern pressure is 135 bar and the minimum cavern pressure is 45 bar.
- Wind turbines are Vestes V164 rated at 7 MW each.
- Wind farm contains 200 wind turbines.
- Air density is assumed constant at 1.2 kg/m³.
- Three stage compression with intercooling and aftercooling for the compressed air energy storage system.
- Two stage compression with intercooling and aftercooling for the compressed hydrogen energy storage system.
- $\eta_{compr} = 75\%$, $\eta_{turb} = 82\%$
- PEM fuel cell system efficiency of 58% (LHV).
- PEM electrolyzer system efficiency of 57% (HHV).
- Electrolyzer H_2 outlet pressure of 13.1 bar.
- Equivalence ratio of 0.4 for the combustion of natural gas [23].
- Combustion turbine operating with 20 bar inlet pressure.
- Sufficient (equipment compressors, turbines, fuel cells, electrolyzers, etc.) with sufficient ramp rates are available to capture excess wind power as well as provide enough power during discharge of storage.

2.4. Model verification

In order to verify the salt cavern model and the compressed air energy storage system model, actual cavern pressure and temperature data for the compressed air energy storage facility in Huntorf, Germany were obtained [32]. Two sets of data

were obtained and utilized to verify the model developed in this paper, one for discharging only (emptying the cavern), and one for the daily operation of charging and discharging the cavern.

The temperature and pressure variations when discharging the cavern were simulated and verified with experimental data. The experimental data was obtained from the Huntorf facility while discharging the cavern from an initial pressure of about 70 bar to a final pressure of about 18 bar during a period of 15 h. The actual air flow rate exiting the cavern at the Huntorf facility was also gathered and used as the input to the model developed in this study. During model calibration, a few parameters were allowed to vary and were subsequently tuned to best fit the experimental data. The pressure and temperature variations presented in Fig. 3 show that the model results agree well with experimental data. The tuned salt cavern parameters used in the model are listed in Table 1.

Note that the compressed air energy storage facility in Huntorf, Germany was the world's first implementation of compressed air energy storage, beginning operation over three decades ago. As explained in the previous section of model components, more recent compressed air energy storage designs have been proposed and implemented in the model. The major differences between our model and the Huntorf design are outlined as follows: 1) newer designs (including our model) have recuperators to increase overall system efficiency; 2) in our model the stored, compressed air is directed to separate, dedicated expanders and not through a combustion turbine; 3) a traditional combustion turbine is used to provide a portion of the power output, and to heat the stored air by means of the recuperator; and 4) a portion of the airflow that exits the high pressure expander is diverted to the combustion turbine to increase its efficiency.

The second set of data collected from the Huntorf facility was for charging and discharging the cavern over a 24-h time period. This data represents the daily operation of the compressed air energy storage system as it both stores and releases energy as needed. Electric grid surplus power, used for air compression (charging the cavern), and power produced by the compressed air energy storage system (when discharging the cavern) was provided by Crotogino et al. [32]. The heat transfer parameters that were verified in the previous cavern model were also used. The proportion of airflow through the combustion turbine, airflow from storage, and airflow for air
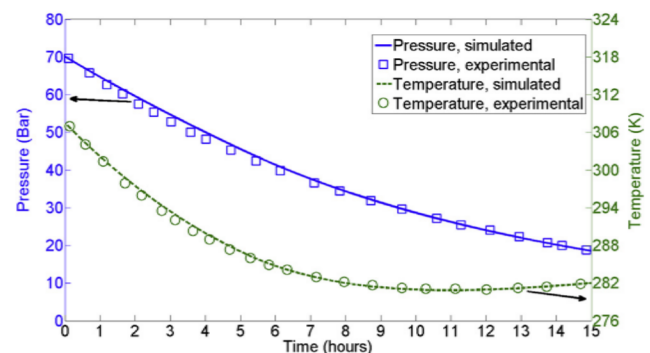

Fig. 3 − Comparison between modeling and experimental data for discharging the cavern.

Table 1 – Salt cavern model parameters.

Parameter	Value
Cavern volume (m^3)	310,000 [32]
Temperature of surrounding bedded salt (K)	318.5
Operating pressure range (bar)	43–70 [32]
Temperature of air entering the cavern after compression and cooling (K)	323
Inner surface area of the cavern (m^2)	43,786
Height of the cavern (sum of both caverns in meters)	310 [32]
Average diameter of the cavern (m)	35.7

injection were adjusted. The isentropic efficiencies of the compressors and turbines were also adjusted to simulate the lower overall efficiency of the older Huntorf facility design. From the comparison shown in Fig. 4, the dynamic model developed was able to capture the pressure variation associated with the Huntorf cavern operation. Actual temperature data was not available, therefore an initial temperature of 330 K was assumed.

The verification process showed that the model developed was able to accurately describe the dynamics associated with the salt cavern. In the next section of this paper various case studies are carried out over a wider range of operating conditions (without changing any of the tuned parameters) and the dynamics associated with the energy storage systems are further discussed.

3. Results and discussion

As stated above, the dynamics of compressed air and hydrogen energy storage technologies integrated with large-scale wind power are key issues to understand their potential performance and impacts on the grid. Therefore, in this paper, compressed air energy storage and compressed hydrogen energy storage systems were simulated and compared; both daily and seasonal load shifting analyses are carried out. Energy storage systems with a small size salt cavern were first investigated (the same cavern size as that of the Huntorf compressed air energy storage facility in Germany [24]). Dynamics associated with power, pressure, and temperature were simulated over the course of one week in early October, 2006. Energy storage systems with a larger size salt
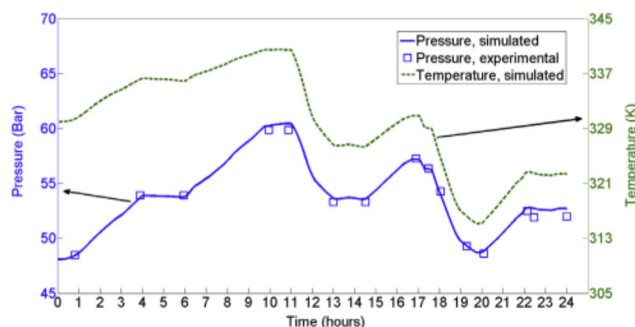
cavern (3.8 million cubic meters) were then investigated for the purpose of seasonal load shifting throughout the entire year of 2006.

3.1. Daily load shifting

Fig. 5 presents the wind power (a wind farm consists of 200 turbines rated at 7 MW each), the grid demand, and the net power in October, 2006. As shown in the figure, net power is the difference between the available wind power and the demand. When the net power is greater than zero it represents the amount of excess wind power that has the potential of being captured and stored. When the net power is less than zero it indicates the power needed from storage (or other sources) to make up for insufficient wind power.

It is assumed that the power plant has sufficient equipment (compressors, turbines, fuel cells, and electrolyzers) to capture and store all excess wind power and to produce all the required power to make up for insufficient wind, provided that the storage cavern is not at its maximum or its minimum pressure. Essentially, in these simplified models, the power plant is capable of always following the exact demand profile, performing perfect load following. However, once the maximum pressure is reached, the facility is no longer able to store energy and all excess wind power is curtailed for as long as the cavern pressure remains at the maximum. If the storage cavern's capacity is completely depleted then the minimum pressure is reached. Once this occurs no power is delivered from storage to make up for insufficient wind for as long as the cavern pressure remains at its minimum. Other load following or peaker plants would have to come online.

In the compressed air energy storage case, it can be seen from Fig. 6 that the cavern is filled to maximum pressure within only a few hours (2.27 h) of operation because of the large amount of wind power available on the first day. For the remainder of the first day and almost the entire second day the wind continues to provide large amounts of excess power, however the cavern is not able to store the vast majority of it. Forty percent of the energy produced by the wind farm must be curtailed during this one week period of early October. The simulation results also show that on October 5th the cavern is rapidly depleted when there is a large decrease in wind power. The cavern pressure drops sharply from maximum pressure all the way to minimum pressure in only 14.3 h, and remains essentially "empty" for almost the entire day on October 6th.
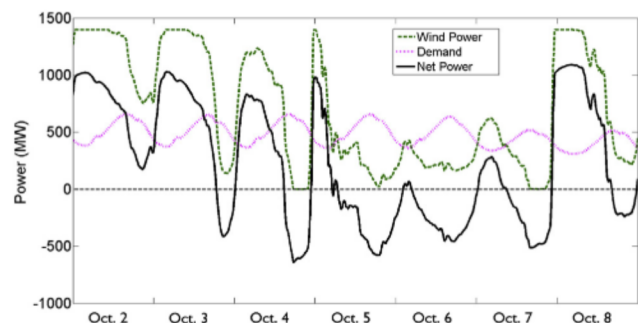

Fig. 4 – **Comparison between modeling and experimental data for the daily operation.**

Fig. 5 – **Power profiles of wind, demand and net power, October 2006.**
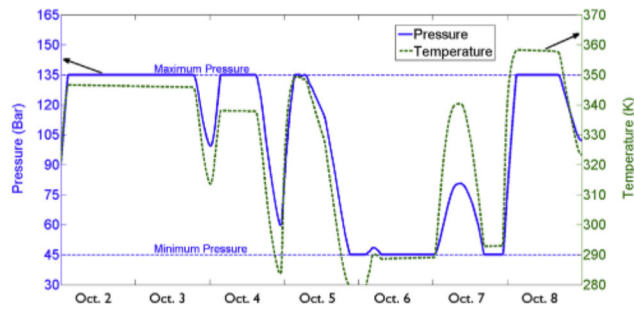
Fig. 6 – **Variations of pressure and temperature inside the carven in compressed air energy storage system.**

Fig. 8 – **Total wind energy and wind energy curtailed for both energy storage systems (H2ES curtailed energy is zero the entire time).**

While the cavern is at the minimum pressure it can no longer provide power from stored wind energy and would have to rely on other generators on the grid. The results indicate that the compressed air energy storage system simulated could not mitigate the intermittency of wind power within the time scale.

As shown in Fig. 7, with the exact same one week period (Oct. 2 through Oct. 8, 2006), as well as the exact same wind power and demand profiles, the compressed hydrogen energy storage system operates within the range of its maximum and minimum pressures. It is noted that no wind energy is curtailed, and the stored wind energy (in the form of hydrogen) supplies all the necessary power during periods when there is a large decrease in wind power. The results indicate that the compressed hydrogen energy storage system simulated could fully utilize the available wind energy and also manage the intermittency introduced.

Compared with the compressed hydrogen energy storage system, the pressure and temperature in the cavern exhibit stronger variations/fluctuations in the compressed air energy storage system. For the same amount of energy to be stored and dispatched, the compressed air energy storage system reaches its limitations much faster than the compressed hydrogen energy storage system, which is attributed to the fact that hydrogen has higher energy density.

The total available wind energy and the amount of curtailed wind energy for both systems over the one week period are also simulated and presented in Fig. 8. As shown in the figure, by the end of the week, the compressed air energy storage system curtailed 46,316 MWh of wind energy (40%),
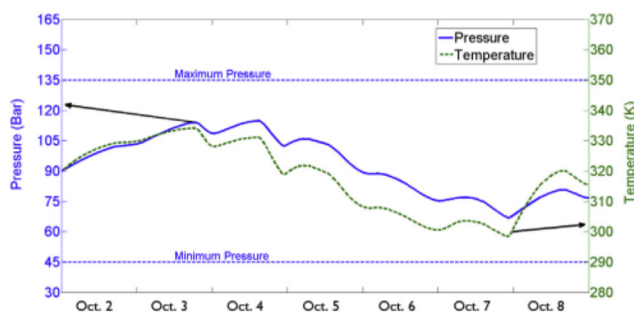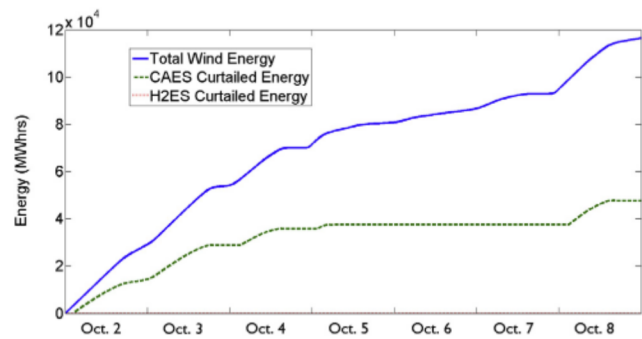
while the compressed hydrogen energy storage system fully utilized all the available wind energy.

In this section, daily load-following simulations were carried out for a wind farm coupled with compressed air and compressed hydrogen energy storage systems while storage cavern temperatures and pressures were simulated. The compressed hydrogen system exhibits much less severe fluctuations in cavern pressure per unit of stored wind energy. With a fixed underground cavern size, hydrogen systems are able to store a greater amount of energy than compressed air systems enabling larger amounts of daily load shifting.

3.2. Seasonal load shifting

To analyze the seasonal load shifting feasibilities of the compressed air and hydrogen energy storage systems, the wind farm with 200 turbines and a salt cavern of 3.8 million m^3 have been implemented in the system models. The demand and daily averaged wind power for the course of 2006 is shown in Fig. 9. As shown in the figure, demand for electricity exhibits a seasonal variation over the course of the year 2006 with peaks in summer, minima in spring and fall. The daily averaged wind power also exhibits seasonal variation with minima in the summer. The monthly averaged wind power in January and August are 945.34 MW and 517.13 MW, respectively. It's noted that such wind power seasonal variation is typical in the U.S. [37]. Estimations of the wind power that could be generated for the contiguous U.S. on a monthly basis have been made by McElroy's group and the results showed that for both onshore and offshore environments, the wind power potential is greatest in winter, peaking in January, lowest in summer, with a minimum in August, and varied over the year by a factor of 2 [38]. It's also noted that the correlation between the monthly averages of wind power production and electricity consumption is negative [38]. Since both wind and electricity demand exhibit seasonal variations, with average wind speeds tending to be lower in the summer while electricity demand is higher, simulations were carried out for an entire year to determine the feasibility of the compressed air and hydrogen energy storage systems for seasonal load shifting. The idea is to gradually store up excess wind energy during the fall and winter months which would then be used to meet the peak energy demands of the summer.
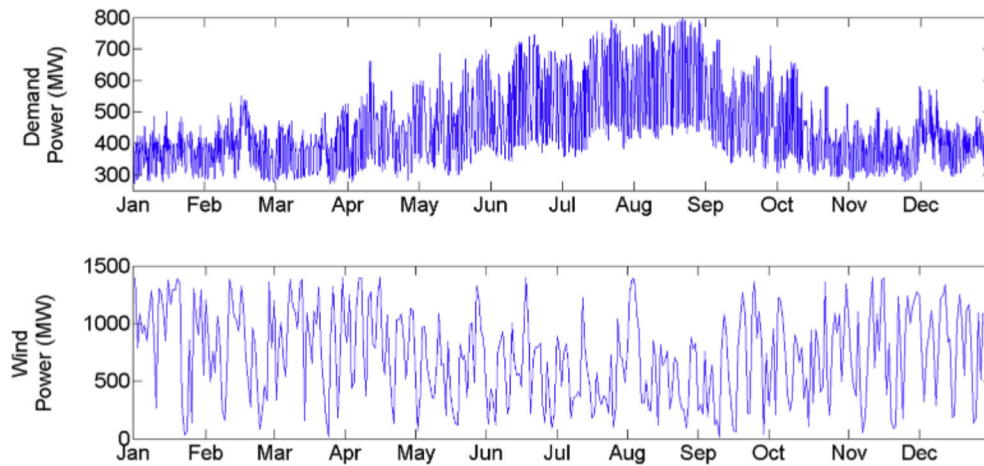

Fig. 7 – **Variations of pressure and temperature inside the carven for the compressed hydrogen energy storage system.**

Fig. 9 − Demand and wind power in 2006.

Three cases with different levels of peak demand (600 MW peak, 800 MW peak, and 1000 MW peak) and identically sized wind farms and caverns have been simulated for the entire year of 2006 for both energy storage systems. Each demand profile is a scaled down version of the demand on the entire ERCOT region in Texas. The cavern pressure and temperature are simulated for both compressed air and compressed hydrogen energy storage systems. Both systems start with a 50% charged cavern.

3.2.1. 600 MW peak demand
Fig. 10 presents the results for the compressed air energy storage system and the compressed hydrogen energy storage

Fig. 10 − Pressure and temperature in the cavern when the peak demand is 600 MW, (A) Compressed air energy storage system and (B) compressed hydrogen energy storage system.

system when the peak demand is 600 MW for one year of operation. Neither system fully utilizes the storage cavern capacity when discharging. It is suggested that the size and the capacity of the cavern could support a larger demand and therefore make more use of the stored wind energy. During charging, the cavern reaches its maximum pressure in both systems. Wind energy is curtailed for both the compressed air energy storage system and the compressed hydrogen energy storage system, however the curtailment begins after only 27 h of operation for the compressed air energy storage system and after 71.7 days for the compressed hydrogen energy storage system. Over the course of the entire year, 53.5% of the total wind energy generated is curtailed due to a lack of storage capacity in the compressed air energy storage system. Only 12.6% of the wind energy must be curtailed in the compressed hydrogen energy storage system during the same (one year) time period.

3.2.2. 800 MW peak demand
Fig. 11 presents the results for both storage systems when the peak demand is 800 MW for one year of operation. The entire capacity of the compressed air energy storage cavern is being utilized, however 38.9% of potential wind energy is curtailed. Moreover, during the months of July and August the cavern occasionally reaches the minimum allowable pressure. Whenever the compressed air energy storage cavern is "empty" it is not able to deliver the energy needed to meet the demand, resulting in a deficiency of approximately 25,000 MWh of energy.

The compressed hydrogen energy storage system curtails only 0.69% of the wind energy and approaches, but does not reach, the minimum cavern pressure in September and October, therefore it almost fully utilizes the storage capacity of the cavern. Seasonal load shifting is accomplished. Excess wind energy from January to April is stored in the cavern and then utilized in June through August as the grid demand reaches its summer-time peak. Fig. 11B clearly shows this storage and release of energy as a gradual increase in cavern pressure through April followed by a gradual decrease in cavern pressure throughout the summer months.
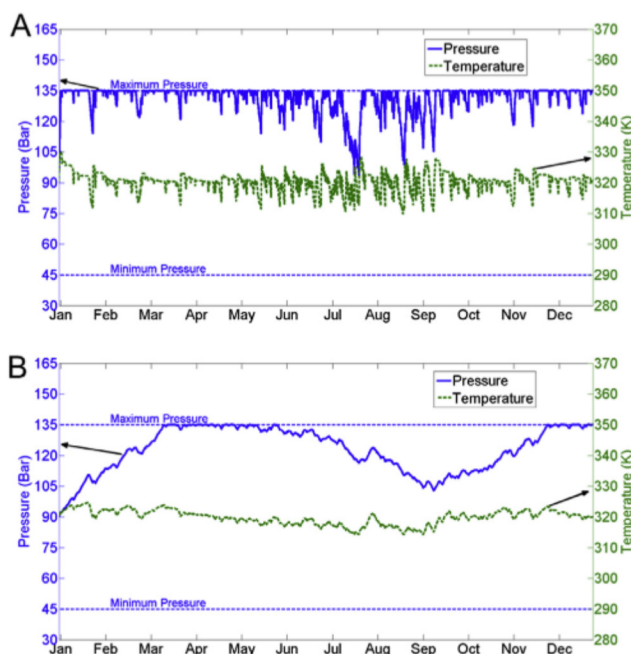
Fig. 11 – Pressure and temperature in the cavern when the peak demand is 800 MW, (A) Compressed air energy storage system and (B) compressed hydrogen energy storage system.

3.2.3.   1000 MW peak demand

Fig. 12 presents the results for both systems when the peak demand is 1000 MW for one year of operation. In this case, the compressed air energy storage cavern again fully utilizes the

Fig. 12 – Pressure and temperature in the cavern when the peak demand is 1000 MW, (A) Compressed air energy storage system and (B) compressed hydrogen energy storage system.
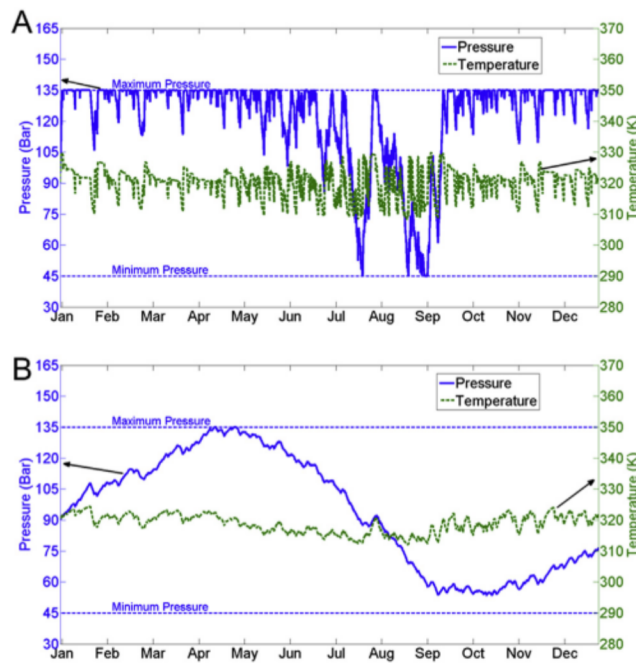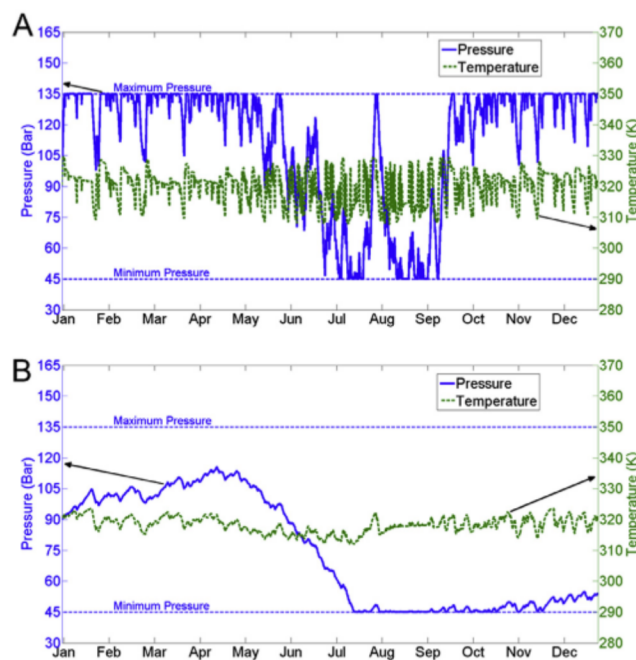
entire storage capacity, however there is 27.4% wind energy curtailment and an energy deficiency of approximately 250,000 MWh over the course of the summer when the cavern is frequently at its minimum pressure. This energy deficiency of 250,000 MWh is 15.8% of the total energy needed from storage (to make up for insufficient wind power) for the entire year.

For compressed hydrogen energy storage, no wind energy is curtailed, however not enough hydrogen is produced during the first four months of the year to provide for the entire summer peak demand. The cavern is completely depleted by mid-July, resulting in an energy production deficiency of about 470,000 MWh, which is 29.7% of the total energy needed from storage for the entire year.

In all three cases, the compressed air energy storage system curtailed about one third or more of the potential wind energy, and it was not able to do seasonal load shifting. The stored wind energy that was utilized during power production mode usually came from the previous few weeks at most. The compressed hydrogen energy storage system had virtually no wind energy curtailment for the 800 and 1000 MW peak cases. For the 600 MW peak case the amount of curtailment, at 12.6%, was still far below even the best case scenario for the compressed air energy storage system.

With the constraints of 200 wind turbines and a cavern size of 3.8 million m³, the compressed hydrogen energy storage system successfully accomplishes seasonal load shifting for the 800 MW peak demand case. A lower demand profile causes wind energy curtailment and does not fully utilize the cavern's storage capacity as can be seen in the 600 MW peak case. On the other hand, a higher demand profile means more of the wind energy is used to meet the instantaneous demand and less is available for storage. This results in the situation where not enough hydrogen is stored to provide for the summer peak (as happens in the 1000 MW peak case). Additional wind turbines would have to be added to the wind farm in this scenario.

For the compressed air energy storage system, none of the three cases presented here are ideal. Wind energy curtailment cannot be avoided, and the cavern cannot provide enough stored energy to mitigate the high summer demand. A much larger cavern would be necessary to accomplish the goal of seasonal load shifting.

It is also important to remember that at least one-third of the power produced by the compressed air energy storage system during power production comes from the natural gas fuel rather than stored wind power. In contrast, the compressed hydrogen energy storage system uses only stored wind energy during power production (or discharge) mode. A wind farm coupled with the compressed hydrogen energy storage system produces 100% clean greenhouse gas-free renewable energy.

In this section, seasonal load-following simulations were carried out for a wind farm coupled with compressed air and compressed hydrogen energy storage systems while storage cavern temperature and pressure dynamics were simulated. It's shown that the compressed hydrogen system exhibits much less severe fluctuations in cavern pressure and that it is able to store a greater amount of energy than a compressed air system with the same cavern size resulting in successful

Table 2 – Wind energy curtailed and round trip efficiency of the two energy storage systems.

Energy storage	Max peak power (MW)	Round trip efficiency	Total wind energy curtailed		Total wind energy losses in conversion		Total energy deficiency	
			GWhrs	%	GWhrs	%	GWhrs	%
Air	600	46.5%	3398.6	53.5%	1582.3	24.9%	0	0%
	800		2475.5	38.9%	2076.7	32.7%	25.2	2.2%
	1000		1744.5	27.4%	2467.9	38.8%	249.4	15.8%
H_2	600	29.9%	797.6	12.6%	3895.9	61.3%	0	0%
	800		43.9	0.7%	4424.9	69.6%	0	0%
	1000		0	0%	4455.7	70.1%	469.8	29.7%

seasonal load shifting for the hydrogen storage system. The seasonal load-following simulation results are also summarized in Table 2. Note that the compressed hydrogen energy storage system curtailed much less wind energy than the compressed air energy storage system, however, the lower round-trip efficiency led to larger losses in the conversion processes of the compressed hydrogen energy storage system.

3.3. H_2 supply pipeline

As stated previously, in a compressed hydrogen energy storage system the hydrogen produced using otherwise curtailed wind power could be dispatched as fuel for zero-emission transportation. One of the major advantages of hydrogen energy storage lies in the fact that the hydrogen can be simultaneously used to mitigate wind power intermittency and provide for seasonal storage, transportation, and distributed generation. This synergistic use of hydrogen allows for the capture of more wind energy than can be accomplished by compressed air energy storage, pumped hydro, or any other renewable energy storage device.

If we reexamine the compressed hydrogen energy storage system with the 600 MW demand peak, we remember that it forced a curtailment of 12.60% of the annual available wind energy. But it would be possible to install a pipeline to carry excess hydrogen to nearby urban centers for use in transportation and distributed generation. When siphoning off a steady supply of hydrogen, the cavern pressure is reduced and curtailment of wind energy can be completely avoided.

As shown in Fig. 13, without the pipeline an excessive amount of hydrogen is produced by the end of the year. With the pipeline, the extra hydrogen is delivered to nearby cities to
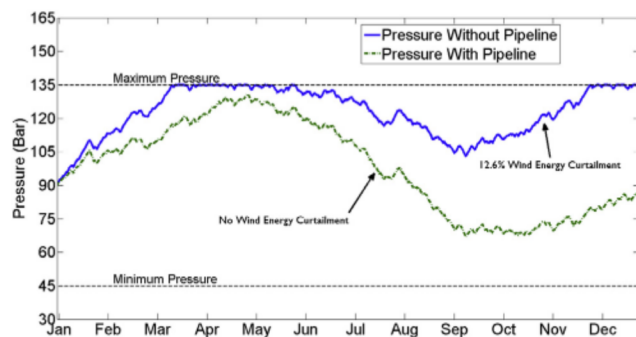
provide fuel for 14,000 fuel cell vehicles per day (assuming an average of 5 kg per vehicle per fill up).

3.4.   Emergency energy reserves

As the number of installed wind farms increases over the coming decades, the likelihood of wind turbine damage due to extreme weather events also increases. Onshore wind farms across the Midwest, as well as offshore wind farms in the Gulf of Mexico and along the East Coast of the U.S. will be particularly vulnerable. Although the Midwest has an abundance of wind energy it is also highly prone to destructive tornados. Likewise, the offshore wind potential of the East Coast and Gulf of Mexico is tempered by the great frequency of hurricanes that pass through these regions. With respect to offshore wind farm damage due to hurricanes, a February 2012 article from the Proceedings of the National Academy of Sciences journal, concludes that, "In the most vulnerable areas now being actively considered by developers, nearly half the turbines in a farm are likely to be destroyed in a 20-yr period [39]." In the event of a damaging tornado, a hurricane, or some other catastrophic interruption in the function of the wind farm, energy storage could provide critical backup power until repairs or replacements could be completed.

Simulations were conducted in order to compare the abilities of several large-scale energy storage systems to provide emergency reserve power in the event of a long term wind farm shut down. It was assumed that each storage facility was at maximum capacity (100% full) when the interruption occurred. It was also assumed that the entire wind farm was damaged or rendered ineffective by the event and therefore zero wind power was being generated. In this situation the stored energy must supply all the power needed to meet the
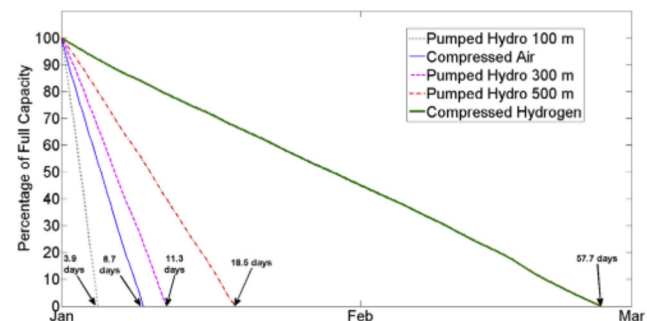

Fig. 13 – Operation of compressed hydrogen energy storage system with and without hydrogen pipeline supporting transportation.

Fig. 14 – Depletion of various large scale energy storage systems while providing emergency backup power.

Table 3 – Energy storage systems providing emergency power.

Energy storage system	Storage type		Storage volume (m³)	Duration of backup power (Days)
Compressed air	Underground cavern		3.8 million	8.7
Compressed H₂	Underground cavern		3.8 million	57.7
Pumped hydro	Two water reservoirs with	100 m head	150 million (each reservoir)	3.9
		300 m head	150 million (each reservoir)	11.3
		500 m head	150 million (each reservoir)	18.5

demand. In addition to compressed gas energy storage, a pumped hydro facility, based on the reservoir sizes at the Helms Pumped Storage Facility in California, was simulated using three different hydraulic heads: 100 m, 300 m, and 500 m.

Fig. 14 (or Table 3) shows the timeframe in which each energy storage system would be depleted. It is clear that the compressed air and pumped hydro systems will only be suitable for relatively short-term backup power. The hydrogen energy storage system provides backup power for the longest duration at 57.7 days, more than three times longer than any of the other systems.

3.5.   Future implementation

Texas has been identified as an ideal location for the compressed gas energy storage facility. The Great Plains of the U.S. could provide enough wind power to supply the energy needs of the nation if it was fully captured and stored [33]. Wind farms in northern Texas as well as in the Gulf of Mexico could be strategically positioned where vast underground salt domes and bedded salt formations are found. Salt caverns can be solution mined for geologic storage of compressed air or hydrogen. Large urban populations such as Oklahoma City, Dallas-Fort Worth, and Houston are nearby. In the case of hydrogen energy storage, hydrogen could be piped to these locations for transportation and distributed generation in fuel cell vehicles and stationary fuel cells, respectively. When high temperature fuel cells that provide combined heating and power (CHP) for buildings are utilized, efficiencies can be greatly improved.

3.6.   Costs

Although it is not the intent of this paper to provide detailed cost comparisons, a few comments are in order. Most economic analyses, based on the current state of technology, show that compressed air energy storage is less expensive

than hydrogen energy storage [37,40]. However when longer duration storage is considered, especially on the order of months (which is necessary for seasonal load shifting and emergency backup power), then hydrogen energy storage has the potential to become the most economically feasible type of storage. When the additional advantages of combined heat and power, as well as, hydrogen that can be utilized as transportation fuel are implemented then the potential economic benefits are even more pronounced, as shown in Table 4 [37].

4.   Summary and conclusions

For the purpose of investigating the transformation of intermittent wind energy into dispatchable power, dynamic models were developed to simulate a wind farm and the electric grid power dynamics together with underground compressed gas energy storage. The compressed gas storage dynamics of the model were verified with experimental data from the compressed air energy storage facility in Huntorf, Germany. Daily and seasonal load following simulations were carried out for a wind farm coupled with compressed air and compressed hydrogen energy storage systems while storage cavern temperatures and pressures were simulated. A separate case was considered in which a pipeline, for the delivery of hydrogen to urban centers, was added to the hydrogen system for the seasonal simulation. Finally, emergency backup power simulations were conducted and the results from three large-scale energy storage systems were compared. The key conclusions of these dynamic system model simulations are as follows:

1) Due to hydrogen's higher energy density, the compressed hydrogen system exhibits much less severe fluctuations in cavern pressure per unit of stored wind energy. With a fixed underground cavern size, hydrogen systems are able to store a greater amount of energy than compressed air systems resulting in less wind energy curtailment and successful daily and seasonal load shifting, even though it has relatively lower round trip efficiency.

2) For seasonal load shifting, the simulated wind farm and storage cavern are most appropriately sized for the 800 MW peak demand profile. Thirty-nine percent of the total annual wind energy is curtailed using compressed air energy storage with this demand profile. Compressed hydrogen energy storage curtails less than one percent of the wind energy for the same demand profile.

3) The addition of a hydrogen pipeline allows the synergistic use of hydrogen for transportation and distributed

Table 4 – Required on-peak electricity prices for a 10% ROI for two months' storage.

Energy storage system	Storage type	Stored electricity price
Compressed air[a]	Underground cavern	185.2 cents/kWh
Compressed H₂[b]	Underground cavern	32.5 cents/kWh

a Storage system efficiency = 90%.
b Electrolyzer HHV efficiency = 87.7%.

generation in addition to load shifting on the electric grid. The storage medium (hydrogen) is completely decoupled from the power conversion devices allowing stored wind energy to be utilized (converted back into electric power) in locations far removed from where it was originally produced. By increasing the possible applications of the stored wind energy, more of it can be captured and utilized which further reduces wind energy curtailment.

4) The simulated hydrogen energy system was able to provide emergency backup power for over six times longer than the compressed air energy system. Again, this can be attributed to hydrogen's higher energy density. The hydrogen system provided emergency power for 57.7 days compared to 8.7 days for compressed air energy storage.

Research and development of electrolyzer and fuel cell technology continues to improve reliability and system efficiencies. If these systems can demonstrate effective power ramping capabilities, then hydrogen energy storage could prove to be a critical component in the management of wind intermittency. Wind farms, along with hydrogen energy storage, could provide clean, renewable, greenhouse gas free energy for both the grid and transportation. Even a modest hydrogen infrastructure for fuel cell vehicles and distributed generation in key U.S. urban regions could alleviate an overtaxed electric grid as plug in battery electric vehicles become an increasing burden. The wind farm and hydrogen storage system would increase the stability of the electric grid by providing dispatchable power while simultaneously reducing the overall load on the electric grid.

Acknowledgements

R E F E R E N C E S

[1] Tarroja B, Mueller F, Eichman JD, Brouwer J, Samuelsen S. Spatial and temporal analysis of electric wind generation intermittency and dynamics. Renewable Energy 2011;36(12):3424–32.

[2] Wiser R, Bolinger M. 2010 Wind technologies market report. Berkeley (CA): Lawrence Berkeley National Laboratory; 2011 Jun. Contract No.: DEAC0205CH11231. Sponsored by the Department of Energy.

[3] Albadi MH, El-Saadany EF. Overview of wind power intermittency impacts on power systems. Electr Power Syst Res 2010;80(6):627–32.

[4] Smith JC, Milligan MR, DeMeo EA, Parsons B. Utility wind integration and operating impact state of the art. IEEE Trans Power Syst 2007;22(3):900–8.

[5] Parsons B, Milligan M, Zavadil B, Brooks D, Kirby B, Dragoon K, et al. Grid impacts of wind power: a summary of recent studies in the united states. Wind Energy 2004;7(2):87–108.

[6] Beaudin M, Zareipour H, Schellenberglabe A, Rosehart W. Energy storage for mitigating the variability of renewable

electricity sources: an updated review. Energy Sustain Dev 2010;14(4):302–14.

[7] Moura PS, De Almeida AT. The role of demand-side management in the grid integration of wind power. Appl Energy 2010;87(8):2581–8.

[8] Kushler M, Vine E, York D. Using energy efficiency to help address electric systems reliability: an initial examination of 2001 experience. Energy 2003;28(4):303–17.

[9] Connolly D, Lund H, Mathiesen BV, Pican E, Leahy M. The technical and economic implications of integrating fluctuating renewable energy using energy storage. Renewable Energy 2012;43:47–60.

[10] Raju M, Khaitan S. Charging dynamics of metal hydride hydrogen storage bed for small wind hybrid systems. Int J Hydrogen Energy 2011;36(17):10797–807.

[11] Díaz-González F, Sumper A, Gomis-Bellmunt O, Villafáfila-Robles R. A review of energy storage technologies for wind power applications. Renewable Sustainable Energy Rev 2012;16(4):2154–71.

[12] Hagen DL, Erdman AG. Flywheels for energy–storage–review with bibliography. Mech Eng 1977;99(7):105.

[13] Pinel P, Cruickshank A, Beausoleil-Morrison I, Wills A. A review of available methods for seasonal storage of solar thermal energy in residential applications. Renewable Sustainable Energy Rev 2011;15(7):3341–59.

[14] Toledo OM, Oliveira Filho D, Diniz ASAC. Distributed photovoltaic generation and energy storage systems: a review. Renewable Sustainable Energy Rev 2010;14(1):506–11.

[15] Khaitan SK, Raju M. Discharge dynamics of coupled fuel cell and metal hydride hydrogen storage bed for small wind hybrid systems. Int J Hydrogen Energy 2012;37(3):2344–52.

[16] Zoulias EI, Lymberopoulos N. Techno-economic analysis of the integration of hydrogen energy technologies in renewable energy-based stand-alone power systems. Renewable Energy 2007;32(4):680–96.

[17] Vosen SR, Keller JO. Hybrid energy storage systems for stand-alone electric power systems: optimization of system performance and cost through control strategies. Int J Hydrogen Energy 1999;24(12):1139–56.

[18] Converse AO. The impact of large-scale energy storage requirements on the choice between electricity and hydrogen as the major energy carrier in a non-fossil renewables-only scenario. Energy Policy 2006;34(18):3374–6.

[19] Denholm P, Kulcinski GL. Life cycle energy requirements and greenhouse gas emissions from large scale energy storage systems. Energy Convers Manag 2004;45(13–14):2153–72.

[20] Desrues T, Ruer J, Marty P, Fourmigué JF. A thermal energy storage process for large scale electric applications. Appl Therm Eng 2010;30(5):425–32.

[21] Steward D, Saur G, Penev M, Ramsden T. Lifecycle cost analysis of hydrogen versus other technologies for electrical energy storage. Golden (CO): National Renewable Energy Laboratory; 2009 Nov. Report No.: NREL/TP56046719. Contract No.: DEAC3608G028308.

[22] Garvey SD. The dynamics of integrated compressed air renewable energy systems. Renewable Energy 2012;39(1):271–92.

[23] Marean JB. Compressed air energy storage engineering and economic study. Final report. Albany (NY): New York State Energy Research and Development Authority; 2009 Dec. Report No.: 1009.

[24] Raju M, Khaitan SK. Modeling and simulation of compressed air storage in caverns: a case study of the Huntorf plant. Appl Energy 2012;89(1):474–81.

[25] Venter RD, Pucher G. Modelling of stationary bulk hydrogen storage systems. Int J Hydrogen Energy 1997;22(8):791–8.

[26] Harrison KW, Martin GD, Ramsden TG. The wind-to-hydrogen project: operational experience, performance testing, and systems integration. Golden (CO): National Renewable Energy Laboratory; 2009 Mar. Report No.: NREL/TP55044082. Contract No.: DEAC3608G028308.

[27] Gonzalez A, McKeogh E, Gallachoir BO. The role of hydrogen in high wind energy penetration electricity systems: the irish case. Renewable Energy 2004;29(4):471–89.

[28] Electric reliability Council of Texas [Internet]. Texas: Electric Reliability Council of Texas, Inc.; [updated 2012 Jul 1; cited 2012 Aug 17]. Available from: http://www.ercot.com/gridinfo/.

[29] Amos W. Costs of storing and transporting hydrogen. Golden (CO): National Renewable Energy Laboratory; 1998 Nov. Report No.: NREL/TP57025106. Contract No.: DEAC3683CH10093.

[30] Stone HBJ, Veldhuis I, Richardson RN. Underground hydrogen storage in the UK. Geol Soc Spec Publ 2009;313:217–26.

[31] Lord AS, Kobos PH, Klise GT, Borns DJ. A life cycle cost analysis framework for geologic storage of hydrogen: a user's tool. Albuquerque (NM): Sandia National Laboratory; 2011 Sep. Report No.: SAND20116221. Contract No.: DEAC0494AL85000.

[32] Crotogino F, Mohmeyer K-U, Scharf R. Huntorf caes: more than 20 years of successful operation. In: Proceedings of SMRI spring meeting 2001 Apr 15–18. p. 15–8. Orlando, Florida, USA.

[33] Leighty W. Running the world on renewables: hydrogen transmission pipelines and firming geologic storage. Int J Energy Res 2008;32(5):408–26.

[34] Li QF, Jensen JO, Savinell RF, Bjerrum NJ. High temperature proton exchange membranes based on polybenzimidazoles for fuel cells. Prog Polym Sci 2009;34(5):449–77.

[35] Debe MK. Advanced cathode catalysts and supports for PEM fuel cells. St. Paul (MN): 3M Company; 2011 May. Contract No.: DEFG3607GO17007. Sponsored by the Department of Energy.

[36] Barbir F, Yazici S. Status and development of pem fuel cell technology. Int J Energy Res 2008;32(5):369–78.

[37] Thomas CE. Energy storage for wind farms. In: Fuel cell Seminar & Exposition 2012 2012 Nov 5-8. [Uncasville, CT, USA].

[38] Lu X, McElroy MB, Kiviluoma J. Global potential for wind-generated electricity. Proc Natl Acad Sci U S A 2009;106(27):10933–8.

[39] Rose S, Jaramillo P, Small MJ, Grossmann I, Apt J. Quantifying the hurricane risk to offshore wind turbines. Proc Natl Acad Sci U S A 2012;109(9):3247–52.

[40] Schoenung S. Economic analysis of large-scale hydrogen storage for renewable utility applications. Albuquerque (NM): Sandia National Laboratory; 2011 Aug. Report No.: SAND20114845. Contract No.: DEAC0494AL85000.